

Impact of Solid Particulate on Brittle Materials

Donato Aquaro

University of Pisa, Department of Mechanical, Nuclear and Production Engineering, Italy

This paper deals with the erosion of brittle materials due to the impact of solid particulate. Erosion tests are characterized by a great uncertainty in the results and high costs. These difficulties led the author to develop alternative methods based on numerical simulations for calculating the erosion rate of brittle and ductile materials. Erosion criteria, based on fracture energy, were developed and implemented as Fortran routines in a commercial FEM code. In this paper the proposed method was applied to calculate the erosion rate of glass and glass ceramics. Fracture energy was obtained using four points bending tests. The numerical results were compared with a developed theoretical model and with the experimental results, available in the literature. In spite of several simplifying assumptions, there was a good agreement between the numerical and experimental results. This method could be a powerful tool for assessing the erosion resistance of components in real operating conditions.

© 2010 Journal of Mechanical Engineering. All rights reserved.

Keywords: erosion model, impact wear, finite element, glass, glass ceramic erosion

0 INTRODUCTION

The erosion mechanism of brittle materials occurs through cracking and chipping and very much depends on the toughness of the material. The maximum erosion rate is obtained with impacts normal to the target (impact angle $\alpha=90^\circ$) [1]. Several theoretical methods have been developed for determining the volume of eroded material as a function of the characteristics of the impacting particles (velocity, radius, density) and of the mechanical properties of the target (hardness, toughness, Young module) [2] and [3].

The functional dependence of the brittle material erosion rate (eroded volume, V , per erodent particle) on the fundamental variables is expressed using the following formula:

$$V = C_1 \omega_p^{e_1} R_p^{e_2} \rho_p^{e_3} K_{C,t}^{e_4} H_t^{e_5} \bar{E}^{e_6} \quad (1)$$

where the exponents e_i depend on the different theories. For the method, developed by the author, (see Appendix I), the exponents are the following:

$$e_1 = 21/10, e_2 = 11/3, e_3 = 21/10, e_4 = -4/3, e_5 = -1/4, e_6 = -8/15.$$

The quantitative value of the eroded volume is calculated knowing the proportionality constant C_1 , which would be material independent and determined by erosion tests. These tests are intrinsically very uncertain. In fact constants for several theoretical approaches, calculated in [2] considering experimental values found in the literature, vary greatly, even though

homogeneous classes of material (ceramics) were used. The greatest difficulty derives from the stochastic characteristics of erosion. Some of the possible causes which influence the variability of the results include the following: the fluid dynamic interaction between the erodent flow and the target, which determines the true value of the velocity vector (direction and magnitude), the actual value of particle energy transmitted to the target, the shielding effects produced by the rebounding of the particles, the actual friction coefficient between particle and target.

Numerical simulations, performed with Finite Element Method (FEM) codes, can describe the erosion mechanisms and can predict the life of components subjected to this phenomenon. The author developed numerical predictive methods [2] and [3] to determine the erosion resistance of brittle and ductile materials. The erosion rate was obtained using numerical simulations of impacts of particulate on the material under examination. Failure criteria, based on the fracture energy, were implemented in a commercial computer code dedicated to the impulsive mechanics [4]. The main hypotheses of the method, applied to brittle materials are :

- erosion is due to a tensile stress state in the elastic regime;
- element damage is assumed to be cumulative and a damage indicator, calculated at each time step and for each element in a tensile stress state represents the eroded fraction of the element at each time step;

*Corr. Author's Address: Dip. Di Ingegneria Meccanica Nucleare e della Produzione, via Diotisalvi n. 2, 56100 Pisa, Italy, aquaro@ing.unipi.it

- an element is considered eroded and eliminated from the mesh when the cumulative deformation energy reaches the value of the fracture energy.

After a brief description of the method reported in detail in [2], the following sections illustrate the determination of the erosion rate of glass and glass ceramics using numerical simulations.

1 THEORETICAL MODEL OF EROSION OF GLASS AND GLASS CERAMICS

Glass and glass ceramic materials are brittle. Glass is an amorphous material characterized by very low values of toughness and ultimate tensile stress. Partial crystallization produces glass ceramics with improved mechanical characteristics. In several applications, these materials are subjected to erosion due to the impact of particles which also degrade their mechanical characteristics.

Our fracture model predicts a cumulative damage in the zones subject to a tensile stress state, while the compressed zones are strengthened due to densification or viscous deformation phenomena and can yield. In the impact, each element is subjected to several cycles of traction and compression due to the transmission and reflection of stress waves on the boundaries. In order to consider this different behavior in tensile and compressive states, the damage variable is calculated as half of the difference between the maximum tensile energy and the maximum compressive energy accumulated in each element during the transient phase. The criterion is equivalent to that used in fatigue resistance calculations. In fact fatigue resistance depends on half of the difference between the maximum and minimum stresses.

In the numerical model, each element is associated with two variables, the first stores the maximum tensile energy and the other the absolute value of the maximum compressive

energy. The damage energy is equal to half of the difference between the previous variables. The fractured element fraction (called "damage"), D_{eli} , is calculated as the ratio between the damage energy and the energy needed to form fracture surfaces. If D_{eli} becomes equal to 1, the element is removed by the mesh. The total eroded mass is determined by multiplying the damage D_{eli} by the element mass and adding it to the mass of all the fractured elements. The model considers the elements in a tensile stress state defined by a positive value of the first invariant stress tensor ($I_1 = \sigma_x + \sigma_y + \sigma_z > 0$) and calculates the element damage function D_{eli} as:

$$D_{eli} = 0.5 \left[\int_{V_{el}} \sigma_{ij}^+ \varepsilon_{ij} dV_{el} - \int_{V_{el}} \sigma_{ij}^- \varepsilon_{ij} dV_{el} \right] / E_{fr} \quad (2)$$

the erosion rate is calculated as:

$$E_{ros_rate} = (\sum \rho_t D_{eli} V_{eli}) / n_p M_p \quad (3)$$

where $\int_{V_{el}} \sigma_{ij}^+ \varepsilon_{ij} dV_{el}$, $\int_{V_{el}} \sigma_{ij}^- \varepsilon_{ij} dV_{el}$ is the

deformation energy, accumulated in the element, due to both a tensile and compressive stress state, respectively; E_{fr} is the fracture energy of the material per unit of volume, V_{eli} is the volume of the element and n_p is the number of erodent particles. If $D_{eli} = 1$, the element is considered eroded and is removed by the mesh. If $D_{eli} < 1$, the element is considered partially eroded. In this case it is assumed that the material strength of the element is reduced. This reduction is taken into account by decreasing the bulk modulus, BM_t , and the shear modulus, G_t , of the material of the partially eroded element using the following expression:

$$BM_{tel}^i = (1 - D_{eli} / D_{elimax}) BM_t$$

$$G_{tel}^i = (1 - D_{eli} / D_{elimax}) G_t$$

$D_{elimax} = 0.7$ in order to avoid numerical instabilities. Differently from [2] and [3], in this application of the fracture model, the degradation

Table 1. Properties of the materials used in the numerical simulations

Material	Bulk modulus [MPa]	Shear modulus [MPa]	Hardness [MPa]	Ultimate tensile stress [MPa]	Fracture energy [J/m ³]	Density [kg/m ³]	Fracture toughness [MPa m ^{0.5}]
Glass	62330	38958	6390	60.9	32224	2200	0.71
Glass Ceramic	71733	43040	8410	197.3	397129	2200	1.72

of mechanical characteristics were not been taken into account during the transient, in order to reduce the complexity of the calculations.

The damage function D_{eli} enables us to implement an erosion model independent of mesh size. In fact the element is eliminated only when the deformation energy of the element is equal to the energy needed to crack the element ($D_{eli} = 1$).

1.1 Characteristics of Glass and Glass Ceramics

The glass and glass ceramics were simulated using a linear equation of state and an elastic plastic constitutive equation in compression. The particle erodent has a spherical geometry ($r = 12.5 \mu$) and is assumed to be rigid.

The mechanical characteristics of the examined materials are reported in Table 1. The material data were obtained from [5]. The glass is made of SiO_2 (80%)- Al_2O_3 - Li_2O using ZrO_2 and TiO_2 as nucleant agents. The glass ceramics was obtained performing partial crystallization of the above mentioned glass. The specific fracture energy was obtained from four-points bending tests on polished samples of glass ($L = 40$ mm; $b = 3.97$ mm; $w = 9.25$ mm) and glass ceramics ($L = 40$ mm; $b = 4.57$ mm; $w = 9.36$ mm) respectively [5].

Fig. 1. shows the load-displacement curves until rupture, which enabled us to calculate the specific fracture energy.

Fig. 2 shows the geometry ($x = 50 \mu$; $y = 100 \mu$; $z = 37.5 \mu$) of the implemented model. Considering the symmetry of the problem only half of the geometry was meshed with 576600

elements. The target was subdivided into two parts: a central zone (control volume, meshed by 375000 cubic elements 0.5μ of side, analyzed for the erosion) and a lateral zone on which the boundary conditions were applied.

Three impact velocities (50, 100 and 150 m/s) were considered. For each case the loading and unloading phase were examined.

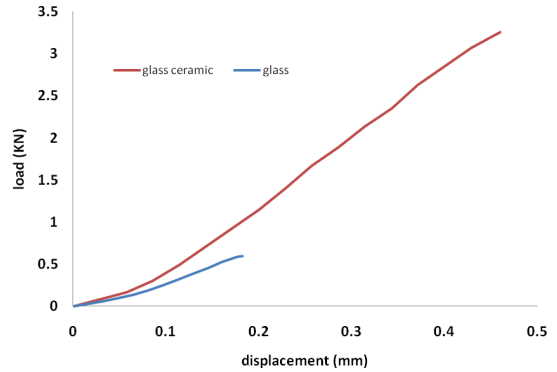


Fig.1. Load versus displacement of glass and glass ceramic in four points bending tests

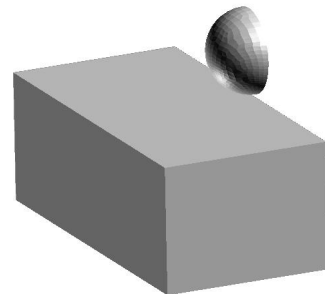


Fig. 2. Model used in the numerical simulation

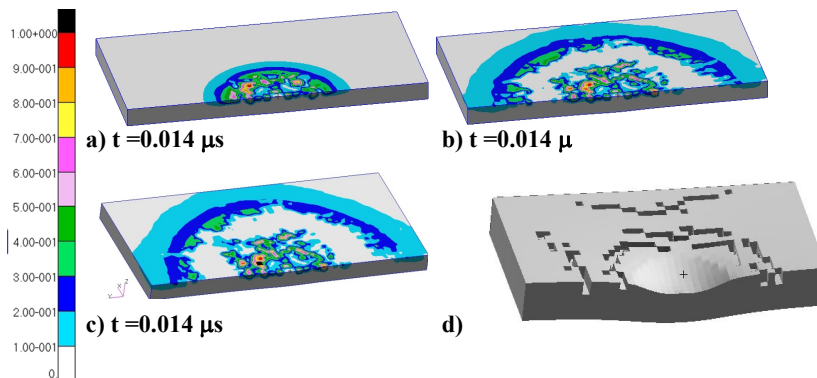


Fig. 3 Distribution of the damage produced by the impact of the particle at 50 m/s against a glass sample and elements eroded around the impacted zone

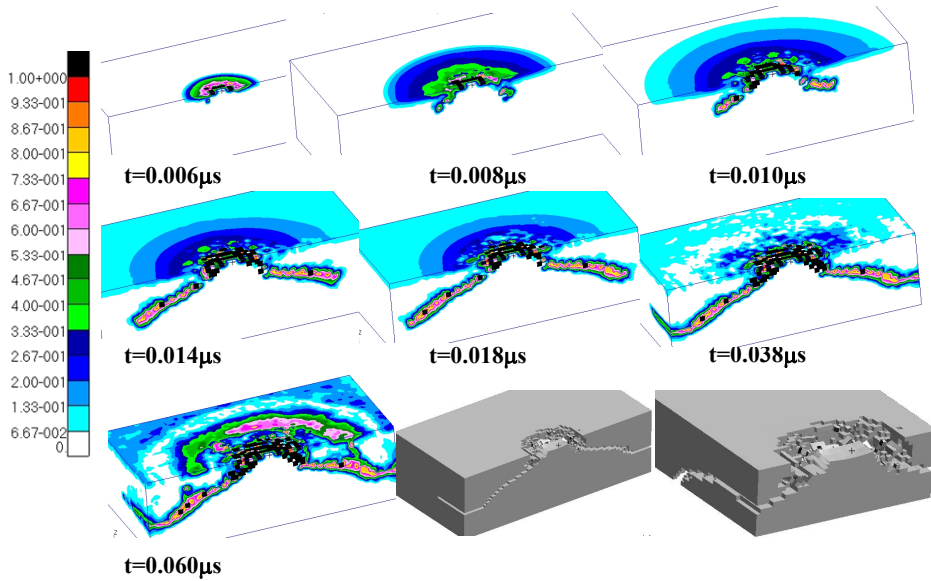


Fig. 4. Distribution of the damage produced by the impact of the particle at 100 m/s against a glass sample and elements eroded around the impacted zone

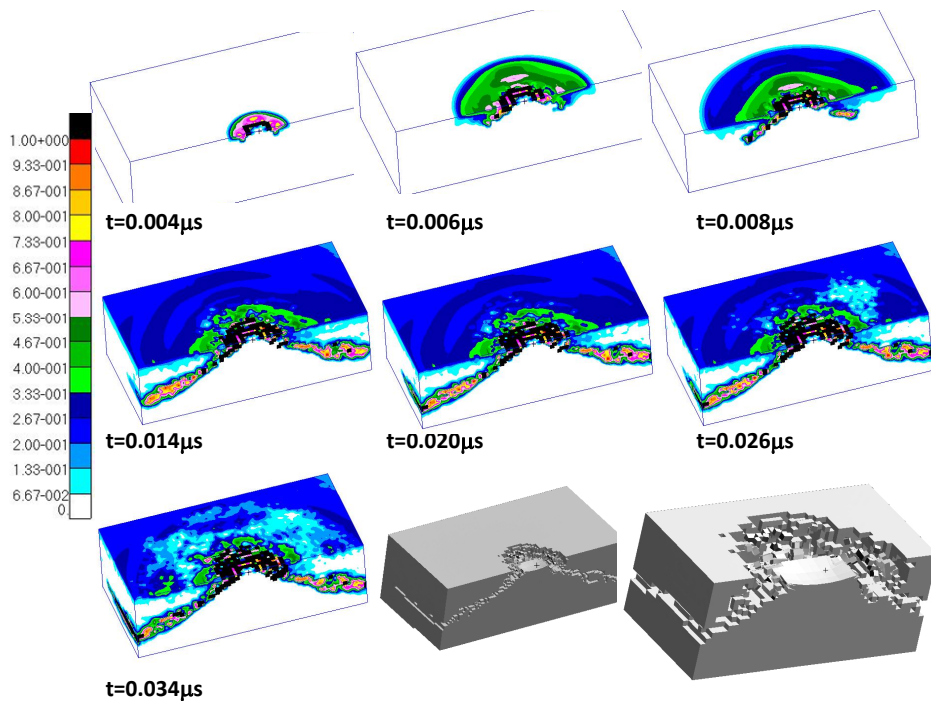


Fig. 5. Distribution of the damage produced by the impact of the particle at 150 m/s against a glass sample and elements eroded around the impacted zone

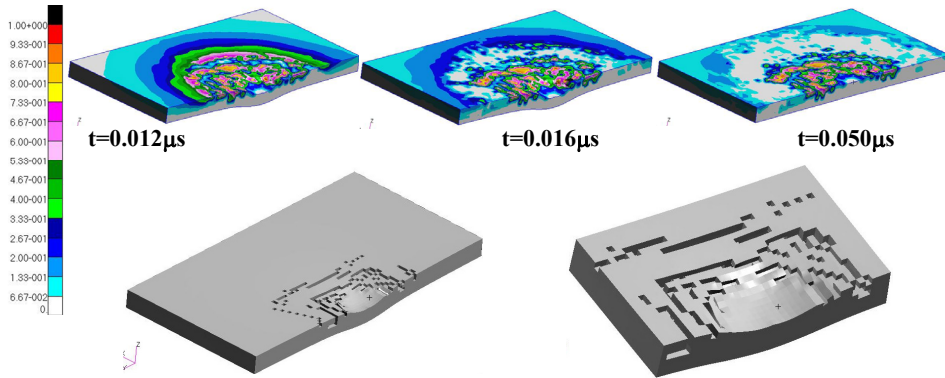


Fig. 6. Distribution of the damage produced by the impact of the particle at 150 m/s against a glass ceramic sample and elements eroded around the impacted zone

2 NUMERICAL RESULTS

Figs. 3 to 6 illustrate the distribution of the damage, D_{eli} on the glass and glass ceramic models, respectively. In addition the spatial distributions of the eroded elements are also shown. The damage morphology is characterized by a compressed central zone, corresponding to the cavity caused by the sphere that penetrates the target and can crush the material underneath. Around the cavity, a high tensile stress produces a fractured collar, which expands in the internal layer to form a fractured conical surface. The extension of the collar and the conical surface depends on the velocity of the impact.

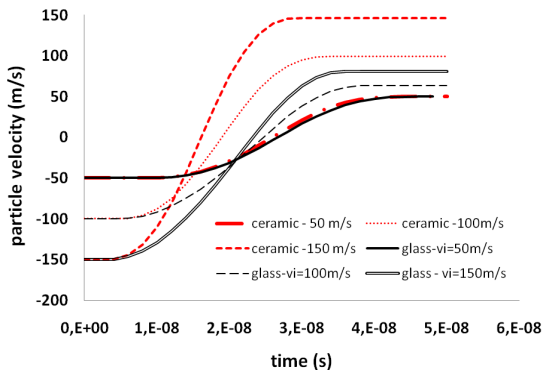


Fig. 7. Velocity of erodent particle versus time

At 50 m/s, only few elements of glass are fractured. These fractured elements are located on the upper surface around the cavity and start in radial direction from it. The conical surface appears at a velocity greater than 50 m/s (Figs. 4

and 5). For impacts on glass with $\omega_p = 50$ m/s, the compression stresses are in elastic regimen and only 0.7% of the energy of the particle erodent is absorbed by the target. This figure becomes approximately 60 and 70% for impact velocities of 100 and 150 m/s, respectively. Glass ceramics have a specific fracture energy than 10 times higher of that of glass and therefore there are eroded elements only for $\omega_p \geq 150$ m/s (Fig. 6). The pattern of the fractured elements of glass ceramic for $\omega_p = 150$ m/s looks like that of glass for $\omega_p = 50$ m/s.

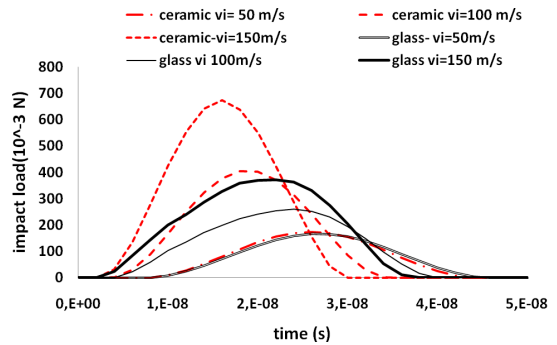


Fig. 8. Load applied by the particle on the target versus time

For lower values of impact velocity, the damage, D_{eli} is lower than 1 in all the elements.

Figs. 7 to 10 illustrate the time histories of the main variables of the erodent particle during the transient. The rebound velocity of the particle is reduced when large erosion occurs ($\omega_p \geq 100$ m/s on glass). In the other case only a small

percentage of the particle kinetic energy is absorbed by the target.

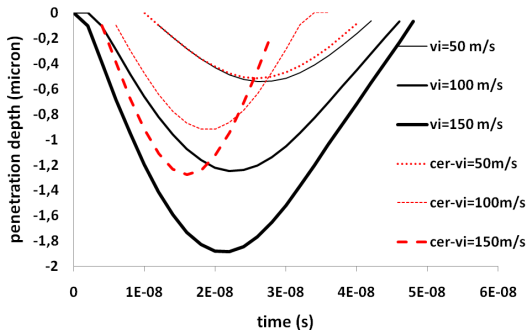


Fig. 9. Penetration depth of the particle into the target versus time

For elastic impacts (impact on glass-ceramic or on glass with $\omega_p \leq 50$ m/s) the load on the target (Fig. 8) is a function of the particle velocity. The maximum values of the force are proportional to $\omega_p^{1.28}$. This agrees with the theory, illustrated in Appendix I, which gives $\omega_p^{1.2}$. In the case of large erosion and plastic behavior under compressive stress ($\omega_p \geq 100$ m/s on glass), the dependence on particle velocity is reduced to $\omega_p^{0.88}$. As the particle is rigid, vertical displacement can be considered as the penetration depth of the particle in the target and enables us to calculate the impact area.

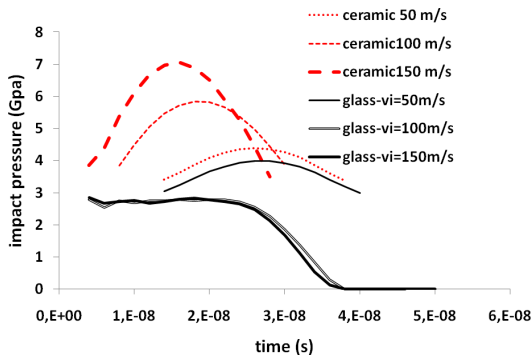


Fig. 10. Pressure on the target versus time

Fig. 9. shows that the maximum value of the particle penetration, in the case of an elastic impact, is proportional to $\omega_p^{0.83}$ which is similar to $\omega_p^{0.8}$ predicted by the theory [2]. In the plastic impact, the penetration is proportional to ω_p . The

penetration depth enables us to calculate the radius of the contact area and the average pressure (Fig. 10). For a plastic impact, the average pressure is independent of the impact velocity and is equal to $0.44S_{yt}$. In the elastic impact is proportional to $\omega_p^{0.42}$.

3 DISCUSSION SECTION: COMPARISON BETWEEN NUMERICAL, THEORETICAL AND EXPERIMENTAL RESULTS

3.1 Comparison Between Numerical and Theoretical Results

Eq. (1), which is derived from the theory in Appendix I, needs the proportionality constant, C_l in order to quantitatively determine the eroded volume. This constant can be determined using the erosion rate calculated by the numerical simulations. The erosion rate is calculated by Eq. (3) and the proportionality constant is obtained dividing this value by the Eq. (1). The theoretical model considers that the fracture occurs in an elastic regimen and depends on fracture toughness, $K_{IC,t}$. In the case under study, the fracture is elastic in the impact against the glass ceramic and against the glass with $\omega_p = 50$ m/s. Therefore the theoretical model correctly applies to these cases. In the impact against the glass with $\omega_p \geq 100$ m/s, the fracture occurs with a yielding in the compressed zones.

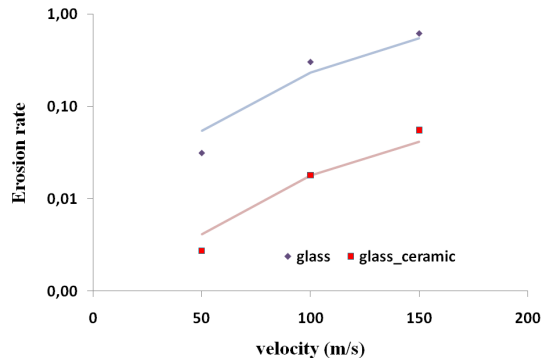


Fig. 11. Erosion rate versus velocity determined by Eq. (1)

Fig. 11 shows the erosion rate curves versus velocity for glass and glass ceramic compared with the numerical values. The curves were obtained by applying the Eq. (1) separately to the two materials and determining the

following constants; glass: $C_l = 0.418 \pm 0.15$; glass ceramic: $C_l = 0.103 \pm 0.034$. The theory is based on elastic fracture and establishes that the constant has to be material independent. The disagreement is due to the high compression stresses which cause the material to yield. It is known [6] that there is a distinction between low-energy and high-energy impact. The damage in the first case is controlled by preexistent surface flaws (i.e. it depends on the fracture energy corresponding to $K_{c,i}$) while in the latter, it is controlled by the cracks produced by the impacting particle (in this case the fracture energy corresponds to the ultimate tensile stress).

The previous considerations demonstrate that the ultimate tensile stress is an important variable in the case of high-energy impact. Therefore Eq. (1) was modified introducing the ultimate tensile stress, σ_u :

$$V = C_2 \omega_p^{e_1} R_p^{e_2} \rho_p^{e_3} K_{c,i}^{e_4} H_i^{e_5} \bar{E}^{e_6} \left(\frac{\sigma_u}{\sigma_u^{ref}} \right) \quad (4)$$

where σ_u^{ref} is a reference ultimate tensile stress.

Fig. 12 shows the erosion rate versus velocity, obtained by applying the Eq. (4) to the glass and glass ceramic, assuming that the reference ultimate tensile stress is that of the glass ceramics. Fig. 12 also reports the numerical results of the erosion rate, normalized to the ratio $(\sigma_u / \sigma_u^{ref})$. The curve in Fig. 12 corresponds to a constant $C_2 = 0.116 \pm 0.04$, obtained considering all the numerical erosion rate results.

3.2 Comparison Between Numerical and Experimental Results

First of all it is interesting to analyze the damage morphology caused by the static indentation of glass produced by a hard sphere. Fig. 13 shows the section profiles of damage patterns, reported in [8]. The damage is due to a detachable collar around the impact area and a cone crack which starts from this collar and extends to the lower layers. In the unloading, median cracks are formed under the impact area. The distribution of fractured elements reported in Figs. 4 and 5 looks like the one shown in Fig. 13. The numerical distribution does not contain median cracks because the crushing, caused by high compressive stresses, was not considered.

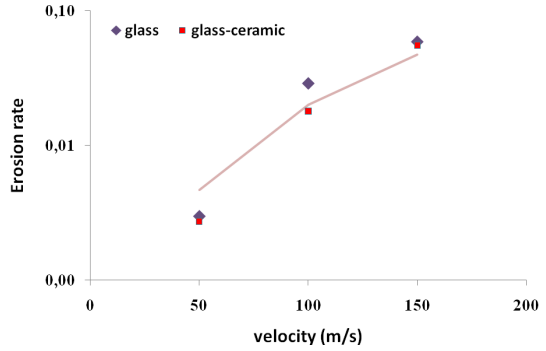


Fig. 12. Erosion rate, normalized to the ratio of the ultimate tensile stresses

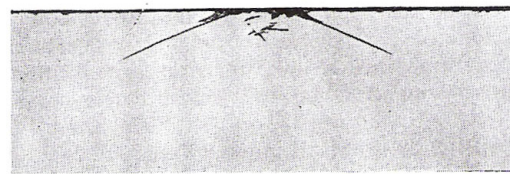


Fig. 13. Damage morphology caused by the static indentation of glass produced by hard sphere [8]

Lawn et al. report in [6] experimental erosion rate data of annealed and tempered glass. The samples were glass disks 50 mm in diameter and 3 mm thick, impacted by SiC grit with a dimension ranging between $37\text{--}300 \mu$ and a velocity up to 120 m/s. The mechanical characteristics of materials are the following:

- Annealed glass $\sigma_u = 121 \text{ MPa}$; $H = 5.7 \text{ MPa}$; $K_c = 0.47 \text{ MPa m}^{0.5}$
- Tempered glass $\sigma_u = 237 \text{ MPa}$; $H = 5.5 \text{ MPa}$; $K_c = 0.47 \text{ MPa m}^{0.5}$

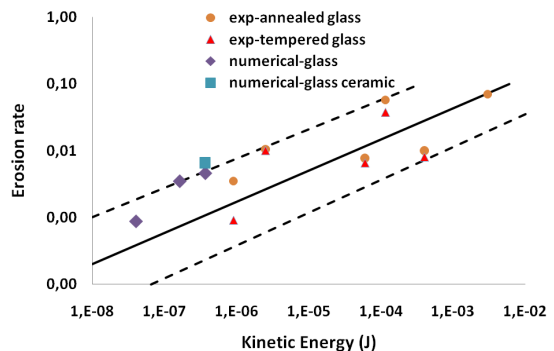


Fig. 14. Comparison between numerical and experimental results [4]

Fig. 14. shows the erosion rate experimental data versus the kinetic energy of

particles and the average curve and the range of variation. The scatter of results is very wide and is typical of erosion tests. The erosion rate experimental data were determined by measuring the weight loss of the target and dividing this value by the weight of particles striking the surface. In order to perform a comparison with the experimental results, only the eroded elements of the upper surface of the numerical model were considered and the values were normalized to the ultimate tensile stress. The comparison is shown in Fig. 14. The numerical values are in the upper part of uncertainty range. This is consistent with the fact that the erodent particle is considered rigid. In the experimental tests, the erodent has sharp edges and therefore some energy was absorbed by the deformation of the erodent.

4 CONCLUSIONS

This paper has illustrated some numerical simulations of the impact of solid particulate against glass and glass ceramic. The main aim of the study was to estimate the erosion resistance of these materials. An erosion model, based on the fracture energy, was implemented in a commercial FEM code dedicated to impulsive dynamic. The behavior of glass and glass ceramics impacted by a rigid sphere at different velocities was simulated. An analysis of the numerical data enabled us to determine the erosion rate. The erosion rates were compared with the experimental results and with the values predicted by a theoretical model. The numerical results agreed well with those of the theoretical model (above all in the elastic impact cases) as well as with the experimental results. Therefore the numerical model would seem to be suitable as a valid tool for determining the erosion resistance of materials.

5 ACKNOWLEDGMENT

The author would like to thank Dr. Papucci who performed the mechanical characterization of the glass and glass ceramic and Prof. M. Papini who implemented the geometrical model.

6 NOMENCLATURE

ν_p	Particle Poisson modulus
ν_t	Target Poisson modulus

E_p	Particle Young modulus [Pa]
E_t	Target Young modulus [Pa]
H_t	Target Hardness [Pa]
$K_{JC,t}$	Target fracture toughness [Pam ^{1/2}]
R_p	Particle radius[m]
ω_p	Particle velocity [m/s]
ρ_p	Particle density [kg/m ³]
ρ_t	Target density [kg/m ³]
M_p	Particle mass [kg]
V	Eroded volume [m ³]
S_{yt}	Target yielding stress [Pa]

$$\bar{E} = (1 - \nu_t^2) / E_t - (1 - \nu_p^2) / E_p (m^2 / N)$$

7 REFERENCES

- [1] Wellman, R.G., Allen, C. (1995) The effects of angle of impact and material properties on the erosion rates of ceramics, *Wear*, vol. 186-187, p. 117-122.
- [2] Aquaro, D. (2006) Erosion Due to the Impact of Solid Particulate of Materials Resistant at High Temperature, *Meccanica*, vol. 41 p. 539-551.
- [3] Aquaro, D., Fontani, E. (2001) Erosion of ductile and brittle materials, *Meccanica*, vol. 36, p. 651-661.
- [4] *MSC-Dytran 2007 r1 - User's Guide* - MSC Software Corporation.
- [5] Papucci, P. (2004) *Determinazione della resistenza alla frattura nei materiali ceramici*, *Tesi di Laurea*, Faculty of Engineering, University of Pisa.
- [6] Lawn, B.R., Marshall, D.B., Wiederhorn, S.M. (1979) Strength degradation of glass impacted with sharp particles: II, Tempered surfaces, *J. Am. Cer. Soc.*, vol. 62, p. 71-74.
- [7] Wiederhorn, S.M., Lawn, B.R. (1979) Strength degradation of glass impacted with sharp particles: I, Annealed surfaces, *J. Am. Cer. Soc.*, vol. 62, p. 66-70.
- [8] Wiederhorn, S.M., Lawn, B.R., (1977) Strength degradation of glass resulting from impact with sphere, *J. Am. Cer. Soc.*, vol. 60, p. 451-458.
- [9] Goldsmith, W. (1960) *Impact- The theory and physical behavior of colliding solids* - Edward Arnold, Publ. London.
- [10] Evans, A.G., Gulden, M.E., Rosenblatt, (1978) Impact damage in brittle materials in the elastic-plastic response regime, *Proc. R. Soc. London A.*, vol. 361, p. 343-365.

APPENDIX I: Theoretical predictive model of the eroded volume by the impact of particles on targets made of brittle materials

The contact force F , between a planar target and a spherical body, based on Hertz's theory [9], is given by the following formula:

$$F = c_2 a^{3/2} \tag{5}$$

where a is called "the approach" i.e. the value of relative displacement along the normal the planar target. It represents the maximum relative compression of the bodies;

$$c_2 = \frac{4R_p^{0.5}}{3D} \quad D = \pi \left[\frac{1 - \nu_t^2}{E_t} + \frac{1 - \nu_p^2}{E_p} \right] = \pi \bar{E}$$

The Hertz contact force can be used to describe the impact between elastic bodies when the vibrations produced by the collision can be ignored. Therefore, Newton's law can be written:

$$F = -\frac{M_t M_p}{M_t + M_p} \ddot{a} = -M_p \ddot{a} \tag{6}$$

We assumed in Eq. (6) that $M_t \gg M_p$. Substituting Eqs. (5) in (6) and multiplying both sides by:

$$\dot{a} = \frac{da}{dt}$$

we obtain:

$$-M_p \dot{a} \ddot{a} = c_2 a^{3/2} \dot{a} \tag{7}$$

Eq. (7) can be written:

$$-M_p \dot{a} d\dot{a} = c_2 a^{3/2} da$$

Then integrating it with the following initial conditions:

$$\text{at } t = 0 \quad a = 0 \quad \text{and} \quad \dot{a} = \omega_p^2$$

we have:

$$-\frac{4c_2 a^{5/2}}{5M_p} = (\dot{a} - \omega_p^2)$$

The maximum approach a_m is obtained when:

$$\dot{a} = 0 \quad \text{and it is equal to} \quad a_m = \left(\frac{5M_p \omega_p^2}{4c_2} \right)^{2/5}$$

Therefore substituting a_m in Eq. (5) we obtain the maximum contact force:

$$F_{\max} = c_2 \left(\frac{5M_p \omega_p^2}{4c_2} \right)^{3/5} = \left(\frac{2000\pi^3 R_p^3 \rho_p^3 \omega_p^6}{243D^2} \right)^{1/5} \tag{8}$$

In Eq. (8) we substituted the expressions of c_2 and $M_p = 4/3\pi R_p^3 \rho_p$.

In the impact of a spherical particle on a brittle material, radial and conical cracks (starting at the boundary of the contact area) develop during the loading phase, while during the unloading phase (the particle rebound) lateral cracks form, starting at the conical cracks and reaching the free surface. Therefore we can assume that the eroded volume V , is proportional to a cylinder volume with a radius equal to c_r (the maximum length of the radial crack) and height equal h_f (the maximum depth of the lateral cracks):

$$V = c_3 \pi c_r h_f \tag{9}$$

where c_3 is a proportionality constant.

Evans has elaborated relations that give :

– the maximum contact force versus c_r and the material toughness K_{Ic} [10]:

$$F_{\max} = c_4 K_{Ic,t} c_r^{3/2} \tag{10}$$

– h_f versus the kinetic energy of the particle and the material hardness H_t [10]:

$$h_f = c_5 \left(\frac{R_p^4 \rho_p \omega_p^2}{H_t} \right)^{1/4} \tag{11}$$

where c_4 and c_5 are constants.

Substituting the Eqs. (8) in (10) and rearranging for c_r , we obtain:

$$c_r = c_4^{-2/3} \left(\frac{2000\pi^3 R_p^{10} \rho_p^3 \omega_p^6}{243D^2} \right)^{2/15} K_{Ic,t}^{-2/3} \tag{12}$$

Substituting the expression of c_r and h_f in Eq. (9) we obtain the expression of the eroded volume:

$$V = C_1 \omega_p^{21/10} R_p^{11/3} \rho_p^{21/10} K_{Ic,t}^{-4/3} H_t^{-1/4} \bar{E}^{-8/15} \tag{13}$$

where:

$$C_1 = \pi c_3 c_4^{-4/3} c_5 \left(\frac{2000\pi^3}{243} \right)^{4/15}$$